

Fluorescence Energy Transfer on Erythrocyte Membranes

H M FUCHS¹, M HOF¹, V MUDOGO² AND R LAWACZECK³

*1 Institute of Physical Chemistry, University of Wurzburg,
Am Hubland D-97074 Wurzburg*

*2 University of Kinshasa Faculty of Sciences,
Kinshasa XI, Zaire*

*3 Institute for Diagnostic Research GmbH at the Free University of Berlin,
Spandauer Damm 130 D-14050 Berlin Germany*

Abstract. Stationary and time-dependent fluorescence were measured for a donor/acceptor (DA) pair bound to membrane proteins of bovine erythrocyte ghosts. The donor *N*-(*p*-(2-benzoxazolyl)phenyl)-maleimide (BMI) and the acceptor fluram bind to SH- and NH₂-residues, respectively. The fluorescence spectra and the time-dependent emission were consistent with radiationless fluorescence energy transfer (RET). Band3 protein is the only membrane spanning protein with accessible SH-groups for the coupling of BMI molecules, and therefore only acceptor binding sites on the same band3 protein were counted by the RET measurements performed. A density of RET-effective acceptor binding sites $c = 0.072 \text{ nm}^{-2}$ was calculated on the basis of the two-dimensional Förster-kinetics.

Key words: Fluorescence resonance energy transfer — Donor-acceptor pair — Förster kinetics — Erythrocytes — Membranes

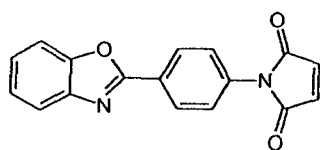
Abbreviations: BMI, *N*-(*p*-(2-benzoxazolyl)phenyl)-maleimide, DA, donor/acceptor, MCA, multichannel analyser, OD (optical density), PMT, photomultiplier tube, RET, resonance energy transfer, TAC, time-to-amplitude converter, SDS, sodium laurylsulphate

Introduction

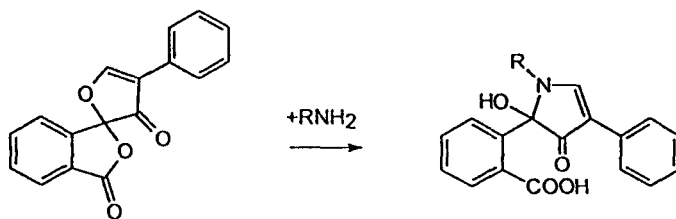
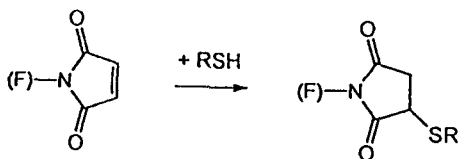
Resonance energy transfer (RET) has become a valuable instrument to look at various phenomena of biological membranes (e.g. Kubitschek et al. 1991; John and Jahnig 1991). Continuing our efforts to understand membrane phenomena we

Correspondence to: R. Lawaczeck, Institut für Diagnostikforschung GmbH an der Freien Universität Berlin, Spandauer Damm 130, D-14050 Berlin, Germany. E-mail: lawaczru@zedat.fu-berlin.de

report herein on resonance energy transfer measurements of a donor/acceptor (DA) pair covalently bound to membrane proteins of red blood cells. RET measurements are suited to follow membrane phenomena like fusion to other particles or induced structural changes. The DA pair discussed was selected in terms of i) easy labeling of the functional groups of proteins, ii) overlapping of the donor fluorescence with the acceptor absorption, and iii) excitation of the donor around 337 nm so that N_2 -laser or N_2 -filled flash-lamps together with the single-photon counting (SPC) technique could be used. N-(p-(2-benzoxazolyl)phenyl)maleimide (BMI) and fluram (fluorescamine) were chosen as donor and acceptor. BMI binds covalently to SH groups (Konoaka et al. 1967) and fluram to NH_2 groups (Bernardo et al. 1974, Stein et al. 1974) (scheme I and II).



I (BMI)



II (FLURAM)

Fluram has the additional advantage that only the bound form fluoresces while the free (non-reacted) molecules are hydrolysed to non-fluorescent products (Bernardo et al. 1974, Stein et al. 1974).

Studies on resonance energy transfer (RET) of fluorescence have also gained attention with respect to fractal structures in non-isotropic media (Even et al 1984, Klafter and Blumen 1984, 1985), which might also be found in biological systems like membranes or cell-interiors. In principle two questions can be answered from RET measurements concerning 1) the distance between labeled positions in macromolecules or in molecular aggregates and 2) the structural dimension of the immediate environment of the donor/acceptor pair. The method has already been utilized successfully for estimating the distance between donor and acceptor molecules and for investigating structural and conformational problems in a large variety of biological macromolecules (Muchte et al 1989, Haran et al 1992, Clegg et al 1993, 1994). Distances are usually determined with respect to the characteristic Forster length, R_0 (Forster 1949), at which the efficiency of the energy transfer is 50%.

In biological systems often only changes of RET efficiency calculated from fluorescence spectra of donor/acceptor pairs are taken as evidence for physiological events (Struck et al 1981). For these studies a few well described RET pairs predominantly coupled to SH- and NH_2 -residues of proteins or lipids are used. In a typical experiment particles containing a donor/acceptor pair at close distance, and thus high RET efficiency, are fused to empty cells or particles. During the course of the fusion events, redistribution of the donor and acceptor molecules over the DA-containing and empty cells takes place. Thus, the average donor/acceptor distance increases resulting in a loss of the transfer efficiency (Lawaczeck et al 1987). In addition to intra- or intermolecular distances, structural information may be obtained from the time dependence of the donor fluorescence. The decay curves serve to determine the spatial dimension of the environment (Even et al 1984, Klafter and Blumen 1984, 1985, Tamai et al 1987). However, a mono-exponential decay curve of the pure donor is required for the extension of the calculations in the direction of the fractal dimensions.

In the following, experiments with DA-labeled red blood cells are described. The experiments were complemented by single cell fluorescence using a microscope spectrometer.

Materials and Methods

Chemicals

Inorganic chemicals of highest available quality were obtained from Merck (Darmstadt, Germany). Chymotrypsin was from Sigma (Deisenhofen, Germany) and sodium laurylsulfate (SDS) from Fluka (Neu-Ulm, Germany). *N*-(*p*-(2-benzoxazolyl)phenyl)-maleimide (BMI) was from Eastman Kodak Comp. (Rochester, USA) and fluram (fluorescamine) from Serva (Heidelberg, Germany). Biogel P10 was obtained from BioRad Laboratories, (Munich, Germany).

Buffers

Buffer A 5 mmol/l sodium phosphate, 150 mmol/l NaCl, pH 7.4

Buffer B 5 mmol/l sodium phosphate, pH 7.4 (for lysis)

Preparation of resealed erythrocyte ghosts

White erythrocyte ghosts, i.e. erythrocytes freed from hemoglobin were prepared according to standard centrifugation procedures (Schwoch and Passow 1978). Usually fresh bovine blood containing fibrinolytic as anticoagulant was washed in isotonic buffer A at 4°C. Lysis was induced by adding buffer B at a volume ratio of 1:4 to 1:6. Hemoglobin was removed by four to five washing steps in hypotonic buffer B. The ghosts were resealed at 4°C overnight in isotonic buffer A.

Labeling

Stock-solutions in acetone of BMI (12 mmol/l) and fluoam (4.3 mmol/l) were prepared separately. In the standard labeling protocol, 50 µl BMI stock-solution was added to 1 ml resealed erythrocyte ghosts (0.1 OD at 400 nm corresponding to about 0.1 mg protein/ml) and incubated at 37°C for 2 h. The unreacted dye was removed by exclusion gel-chromatography (Biogel P10). The acceptor fluoam was added shortly before the actual fluorescence measurements. As the unreacted fluoam molecules are hydrolysed to a non-fluorescent product no separation of the unreacted dye was necessary.

Fluorescence and absorption measurements

Stationary fluorescence and absorption spectra were recorded with an SPF 500 fluorescence spectrometer (American Instrument Company) and a UV 5260 spectrophotometer (Beckman Instruments), respectively. Usually, rather dilute solutions were measured to avoid straylight and inner-filter effects. For microscopic observations of the labeled ghosts a Zeiss UEM fluorescence microscope equipped with a spectrometer accessory was used.

Fluorescence lifetimes were determined by using time-correlated single-photon counting technique. All decay measurements were performed under single photon counting conditions. The flash lamp was thyatron-triggered (Applied Photophysics Ltd. model 435/012) air-filled and run at 20 kHz with 4 kV applied across a 1.5 mm electrode gap. The half-width of the pulse was about 2.5 ns. The excitation and emission wavelengths of 337 nm and 366 nm, respectively, were selected by Ortel interference filters. Emission was detected by using an RCA 850, 12 stage photomultiplier tube (PMT). Single photon pulses of the PMT were used as "stop" pulses for the Ortel model 457 time-to-amplitude converter (TAC). The "start" pulses for the TAC were obtained from a RCA 1P28 PMT which was attached to the lamp housing. The "start" and "stop" pulses were routed through constant

fraction discriminators (Ortec models 473a and 583) in order to improve the signal-to-noise ratio. The output of the TAC was stored in a multichannel analyser (MCA, Norland/Ino-Tech model 5400). The time calibration of the TAC-MCA combination was performed with an Ortec delay model 425a. Electromagnetic interference was eliminated by covering the cables, the lamp- and photomultiplier-housing with copper shields. Single-point grounding was used. To measure the total fluorescence intensity, the polarizer in the emission light path was set at the magic angle of 54.7° .

Data analysis

The observed fluorescence decay curve $R(t)$ is represented by the convolution integral

$$R(t) = \int_0^t G(t')F(t-t')dt' \quad (1)$$

where $G(t)$ is the apparatus response function and $F(t)$ is the true fluorescence decay. The true (unknown) fluorescence decay was calculated by fitting a theoretical fluorescence decay $R'(t)$ to the experimental data $R(t)$ using the least squares iterative deconvolution technique. The χ^2 values and the plots of the weighted residuals $r(t)$ served to characterize the accuracy of the fit (Büch and Imhof 1985) (see Fig. 4). Excellent agreement with the published lifetimes for standard fluorophores and χ^2 values close to unity were obtained. Details of the convolution procedure have already been described (Hof et al. 1989).

Functional test

The intactness of the anion-ion exchange system (functional units of the band 3 protein) of the erythrocyte ghosts (labeled or unlabeled) was verified on the basis of anion-dependent proton-transfer experiments (Pitterich and Lawaczeck 1985). The labeling with the donor molecules, BMI, did not alter the transfer kinetics.

Results

Completely white and resealed ghosts at a protein concentration of 0.1 mg/ml (corresponding to a turbidity of 0.1 OD at 400 nm) were first labeled with BMI. The unreacted BMI molecules were removed by gel chromatography as described above. 20 to 160 μ l flouam was added to the BMI-labeled ghosts (in 2 ml of buffer A) just prior to the fluorescence measurements. In control experiments flouam was added to ghosts without BMI. In Fig. 1 typical emission spectra of these experiments are reproduced. As free flouam is hydrolysed to non-fluorescent molecules (Bernardo et al. 1974, Stein et al. 1974) a second separation step is not necessary. It is obvious from Fig. 1 that the increasing amounts of the acceptor flouam led to an increase of the acceptor fluorescence at the expense of the donor signal. Emission maxima

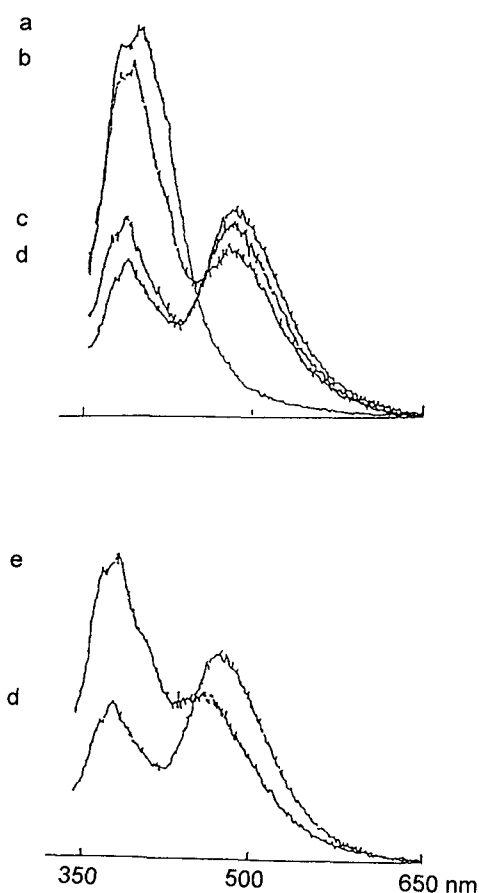


Figure 1. Fluorescence spectra of erythrocyte ghosts labeled with BMI (donor) in the absence (a) and presence (spectra b to d) of 0.8 , 2 and 5.6×10^{-4} mol/l flouam (acceptor) respectively. In the lower panel erythrocyte ghosts were labeled with BMI and flouam (5.6×10^{-4} mol/l same as spectrum d) and subsequently solubilized by the addition of the detergent SDS (spectrum e). Excitation at 337 nm (donor excitation) and emission from 350 to 650 nm. Measurements were carried out at room temperature. The peak centered at 375 nm corresponds to the donor emission and the peak at 475 nm to the acceptor emission, respectively.

for the donor and the acceptor were 360/378 nm and 475 nm, respectively. Flouam alone also fluoresced if excited at 337 nm, i.e. at the donor excitation wavelength, but less than in the presence of the donor BMI. The addition of an ionic detergent (SDS) solubilized the membrane and destroyed the transfer efficiency culminating in an increase of the donor and a decrease of the acceptor fluorescence. The digestion of the external membrane proteins by chymotrypsin led to similar results.

The above trends are typical for RET experiments on membrane bound donor/acceptor pairs. In the case of the erythrocyte membrane the binding site of externally added SH-reagents like BMI is attributed to the band 3 protein, which is the major membrane spanning protein (Cabantchik et al. 1978)¹⁾. The second major

¹⁾ The proteins of erythrocyte membranes are numbered according to the pattern of gel electrophoresis.

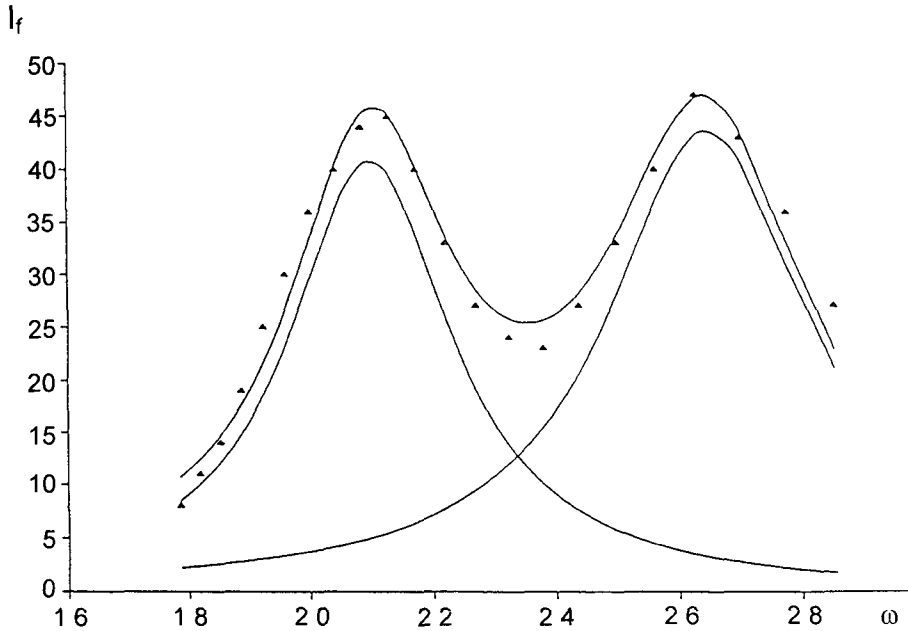


Figure 2. Spectrum c from Fig. 1 decomposed into two Lorentzian lines according to

$$I_f = \frac{f_1}{(\omega - \omega_1)^2 + (\Gamma_1/2)^2} + \frac{f_2}{(\omega - \omega_2)^2 + (\Gamma_2/2)^2}$$

Experimental fluorescence intensity I_f in arbitrary units versus $\frac{1000}{\lambda}$ together with the individual and the sum of the two Lorentz lines. For each calculation ω was set to $\frac{1000}{\lambda}$ (with λ in nm). Results

$$f_1 = 1.75 \quad \omega_1 = 2.65 \quad \Gamma_1 = 0.40$$

$$f_2 = 1.06 \quad \omega_2 = 2.10 \quad \Gamma_2 = 0.32$$

(ω, Γ in units of $\frac{1000}{\lambda}$ with λ in nm)

membrane spanning protein, glycoprotein, does not contain accessible SH-groups and can therefore be excluded as a binding site for the donor molecules.

Since the donor/acceptor-peaks show an overlapping region the spectra were decomposed into two Lorentz-curves (Fig. 2) using a Marquardt-Levenberg algorithm. From these Lorentz-intensities relative quantum yields $\phi_r = \phi_{DA}/\phi_D$ were calculated with ϕ_{DA} and ϕ_D the quantum yields in the presence and the absence of acceptor molecules, respectively. In Fig. 3 these relative quantum yields were

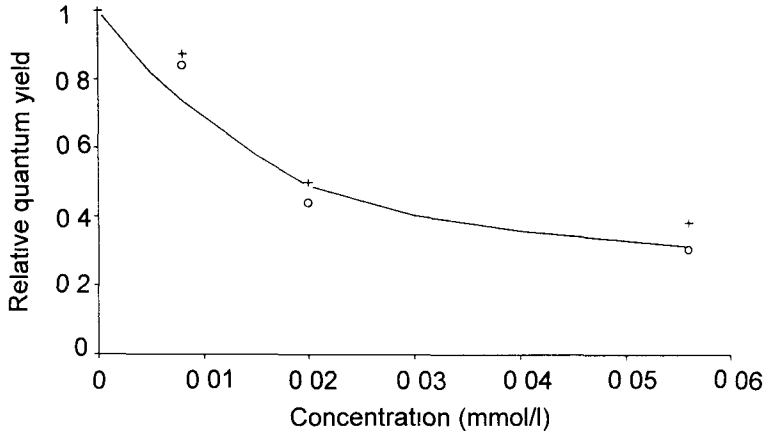


Figure 3 Relative fluorescence quantum yields $\phi_r = \phi_{DA}/\phi_D$ as function of the stoichiometric acceptor concentration c_0 (+) experimental values (o) maximal values from the Lorentz functions (see Fig. 2)

plotted as function of the initial acceptor concentration c_0 ²⁾

Further information on the system can be achieved from time-dependent measurements. For that purpose the following set of samples was prepared and measured (excitation at 337 nm, emission at 366 nm, 20°C): a) free BMI, b) BMI bound to erythrocyte ghosts, c) sample b after 12 h, d) BMI bound to erythrocyte ghosts with the acceptor fluram, e) sample d subsequent to the addition of SDS, and f) sample d after adding chymotrypsin. Fig. 4 shows a typical result of these measurements together with the decay curve fitted according to a deconvolution on the basis of mono-exponential fluorescence decay function. The residual plot and the χ^2 value were also included in Fig. 4.

The binding of BMI to the membrane proteins led to an increase of the fluorescence lifetime compared with free BMI. The slight shortening of the fluorescence lifetime observed after 12 h is possibly due to a rearrangement of the membrane constituents. The addition of the acceptor molecule reduced the fluorescence lifetime and led to a decrease of the signal-to-noise ratio as a consequence of the reduced donor fluorescence (see Fig. 1). This effect was almost abolished by solubilization of the membrane or by enzymatic cleavage of the membrane proteins. The obtained fluorescence lifetimes are summarized in Table 1. The decay curves of the pure acceptor could not be adequately measured at the excitation and emission wavelengths of 337 nm and 366 nm, respectively, due to the low signal intensities.

²⁾ From these plots effective acceptor densities can be calculated (Wolber and Hudson 1979) for the case of a two-dimensional radiationless dipole-dipole interaction (Forster mechanism).

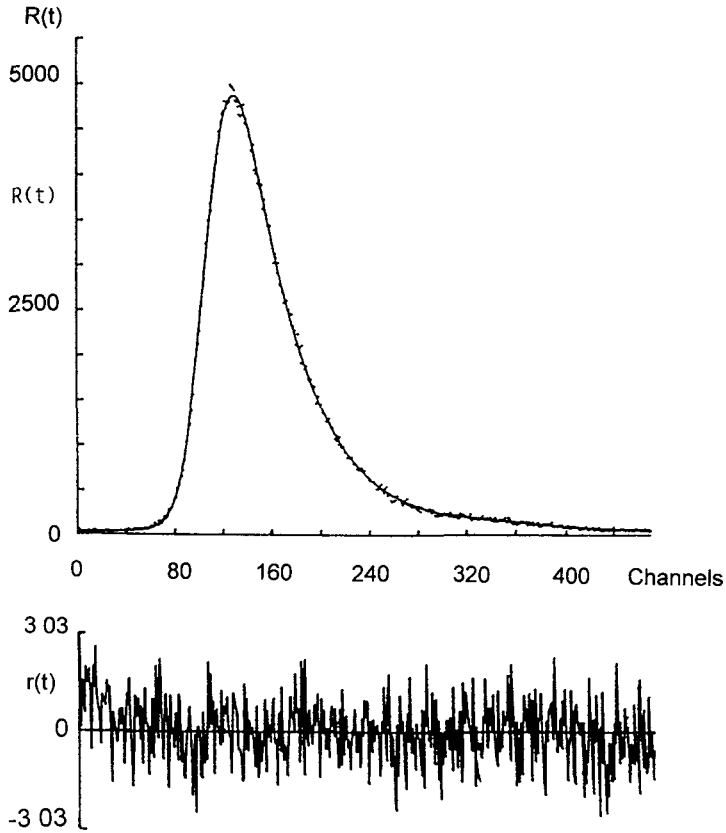


Figure 4. Time-dependent emission decay. Experimental $R(t)$ and calculated $R'(t)$ emission decays for erythrocyte ghosts labeled with the donor BMI in the absence of the acceptor versus channel number (1 channel corresponds to 0.0213 ns) together with the residual plot $r(t)$ on the basis of mono-exponential decay ($\tau = 1.13$ ns, $\chi^2 = 0.95$). $T = 20^\circ\text{C}$, excitation 337 nm, emission 366 nm. $r(t)$ and χ^2 are defined according to

$$\chi^2 = \sum_{i=1}^N \frac{[R'(t_i) - R(t_i)]^2}{R'(t_i)} \frac{1}{N - n - 1} \quad r(t) = \frac{[R'(t_i) - R(t_i)]}{R'(t_i)}$$

with the number of data points N and the number of fit-parameters n respectively.

under these experimental conditions and a rather short fluorescence lifetime.

The decay curves of the donor fluorescence (sample a, b, c) can reasonably be fitted by mono-exponential decay functions with χ^2 -values close to 1 in contrast to samples where both the donor and the acceptor were present (e.g. sample d).

Table 1. Average fluorescence lifetimes τ (ns) calculated on the basis of a mono-exponential decay function*

Samples	τ (ns)
BMI free	0.97 ± 0.08
BMI bound to erythrocyte ghosts	1.13 ± 0.10
BMI bound to erythrocyte ghosts after 12 h	1.07 ± 0.05
BMI bound to erythrocyte ghosts after the addition of 10^{-4} mol/l fluram	0.83 ± 0.05
BMI bound to erythrocyte ghosts after the addition of 10^{-4} mol/l fluram followed by the addition of chymotrypsin	1.09 ± 0.05
BMI bound to erythrocyte ghosts after the addition of 10^{-4} mol/l fluram followed by the addition of SDS	0.99 ± 0.03

*For systems in the absence of acceptor molecules the χ^2 -values are between 0.95 and 1.10. In the presence of acceptor molecules, these values are slightly larger but do not exceed 1.25. For chymotrypsin and SDS studies three experiments and for all other cases six independent measurements were averaged, respectively.

Table 2. Results of time-dependent fluorescence measurements with a deconvolution based on the Förster-kinetics with different dimensions (lifetime $\tau = 1.13$ ns (pure donor)) χ^2 -values and γ (according to eq. (2))

	χ^2	γ
Mono-exponential fit	1.25	-
Three dimensions $\beta = 1/2$	1.17	0.79
Two dimensions $\beta = 1/3$	1.05	1.23

The data for sample d were therefore subjected to deconvolution according to the generalized Förster-kinetics (radiationless dipole-dipole energy transfer) in three and two dimensions (Hauser et al. 1976):

$$F(t) = A \exp[-t/\tau - \gamma (t/\tau)^\beta] \quad (2)$$

with an amplitude factor A . τ is the fluorescence lifetime of the pure donor, and $\beta = D/6$ for weak dipole-dipole interaction with D being the dimension of the system in question. γ is a constant factor determined by R_0 , D and the effective density of acceptor molecules, c . The results of these calculations are listed in Table 2.

The change from mono-exponential to the Förster-kinetics leads to an improvement of the fit manifested in the χ^2 -values. From these fits information concerning

the dimension (parameter β) of the energy transfer and the surface concentration c is available. For the two-dimensional case ($\beta = 2/6$), which seems most appropriate, γ is given by (Wolber and Hudson 1979)

$$\gamma \approx 4.25 R_0^2 c \quad (3)$$

$R_0 = 2$ nm was separately determined from measurements of the intramolecular energy transfer between BMI and fluoam. For that purpose, small peptides with BMI and fluoam coupled to the end groups had been synthesized and characterized by RET methods (Hof 1990). On the basis of $R_0 = 2$ nm and a γ -value of 1.23 one calculates the two-dimensional density of acceptor molecules to be 0.072 nm^{-2} .

Discussion

The above results reveal that RET measurements yield valuable information concerning the donor-acceptor interactions on membraneous systems. The donor BMI, added externally, is predominantly coupled to SH-residues of cysteines from the band3 proteins. Band3 protein is the major membrane spanning protein with SH-residues accessible from the external side. The acceptor fluoam binds to NH_2 -groups, and only the bound form contributes to the fluorescence emission. The exact concentrations of both the donor and the acceptor on the membrane cannot be obtained from standard UV/VIS absorption and emission measurements because contributions from the aromatic amino acids and from the light scattering of the erythrocyte ghosts cannot be excluded.

On the basis of the above stationary and time dependent measurements an estimate of the acceptor surface concentration is possible. The effective two-dimensional density of acceptors is 0.072 nm^{-2} . If the acceptor was homogeneously distributed over the membrane surface of $90 \times 10^6 \text{ nm}^2$, 6.5×10^6 binding sites per membrane surface would be calculated. For band3 protein the number of copies per red blood cell are in the order of one million copies per cell (Steck 1974). The calculated number of effective acceptor binding sites is in the order of the band3 protein copies. However, this figure overestimates the number of band3 proteins as they must share the membrane surface with lipid molecules and other proteins like glycoproteins. Further, even if not all 6 SH-groups on a single band3 protein are accessible, the stoichiometric labeling could be in excess of 1:1 (for purified band3 Rao et al. (1979) reported numbers between 1.4–2 BMI per band3 molecule). Both arguments emphasize that the number of band3 proteins per red blood cell calculated on the basis of the above two-dimensional Förster-kinetics must be considered as an upper limit. "Effective" under the present conditions refers to "taking part in the radiationless energy transfer from donor to acceptor". As the RET efficiency reflects the donor-acceptor distance, acceptor binding sites different from band3

protein (e.g. glycophorin) are not counted by the method employed. Solubilization of the membrane by detergents or cleavage of the membrane proteins into fragments increase the DA distances in parallel with a decrease of the RET efficiency.

Previously BMI has been used to map the distance from the BMI binding site to the binding site of stilbene derivatives which are known as specific inhibitors of the anion-exchange of the functional band 3 units (Cabantchik et al. 1978). R_0 values around 2.9 nm for the BMI stilbene system and lifetimes ($\tau = 0.88$ and 0.70 ns at 23°C in the absence and the presence of the stilbene-derivatives respectively) have been determined (Rao et al. 1979). Though these τ values are slightly shorter they are consistent with our values from Table 1. Our data further reveal that the binding of BMI to the membrane increases the fluorescence lifetime while subsequent addition of the acceptor leads to a life time reduction. The BMI-fluorim system has the obvious advantage of an easy handling devoid of complex reaction conditions. The small overlapping of the donor and acceptor emission can be tolerated. For quantitative purposes, however, it seems reasonable to decompose the recorded fluorescence spectra into two Lorentzians.

For mono-exponential decay of the donor fluorescence like in the present case for BMI bound to proteins on erythrocytes additional progress in terms of structural information is possible. In the present case the Förster kinetics in three and two dimensions were implanted in the deconvolution procedure and Table 2 indicates that the computational fit is better for two than for three dimensions. This result seems reasonable for donor/acceptor pairs located on membrane surfaces. However, it seems premature at the present stage to include further reaching concepts in the data analysis.

Microscopic observations revealed violet/blue fluorescence from the labeled erythrocyte ghosts. Most of the ghosts are of discoid shape with minor echinocyte contributions. There is no change in shape of the ghosts by going from BMI/fluorim labels discussed here to other RET pairs or fluorophores like 6-(7-nitrobenz-2-oxa-1,3-diazol-4-yl)amino hexan acid/rhodamine or fluorescein.

Conclusion

The donor/acceptor pair described is suited for resonance energy transfer studies on membranous systems. Both the donor and the acceptor carry coupling groups for the labeling of accessible SH- or NH_2 -residues of membrane proteins. The labeling is performed by adding the donor/acceptor molecules to aqueous solution containing the cells or membranes to be studied. No separating step removing the unreacted acceptor is necessary since the unreacted acceptor molecules are hydrolysed to non fluorescent products. In the present case the fluorescence energy transfer can appropriately be described by a two-dimensional Förster-kinetics allowing the calculation of the acceptor density in the proximity of the donor molecules.

References

- Beinardo de S, Weigele M, Toome V, Manhart K, Lemgiuber W, Bohlen P, Stein S, Udenfriend S (1974) Studies on the reaction of fluorescamine with primary amines *Arch Biochem Biophys* **163**, 390—399
- Birch D J S, Imhof R E (1985) Kinetic interpretation of fluorescence decays *Anal Instrumentation* **14**, 293—329
- Cabantchik Z I, Knauf P A, Rothstein A (1978) The anion transport system of the red blood cell. The role of membrane protein evaluated by the use of 'probes' *Biochim Biophys Acta* **515**, 239—302
- Clegg R M, Murchie A I H, Zechel A, Lilley D M J (1993) Observing the helical geometry of double-stranded DNA in solution by fluorescence energy transfer *Proc Natl Acad Sci USA* **90**, 2994—2998
- Clegg R M, Murchie A I H, Lilley D M J (1994) The solution structure of the four-way DNA junction at low-salt conditions: a fluorescence resonance energy transfer analysis *Biochem Biophys J* **66**, 99—109
- Even U, Rademann K, Jortner J, Manor N, Reisfeld R (1984) Electronic energy transfer on fractals *Phys Rev Lett* **52**, 2164—2167
- Forster T (1949) Experimentelle und theoretische Untersuchung des zwischenmolekularen Ubergangs von Elektronenanregungsenergie *Z Naturforsch* **4A**, 321—327
- Haran G, Haas E, Szpikowska B K, Mas M T (1992) Domain motions in phosphoglycerate kinase: determination of interdomain distance distributions by site-specific labeling and time-resolved fluorescence energy transfer *Proc Natl Acad Sci USA* **89**, 11764—11768
- Hauser M, Klem U K A, Gosele U (1976) Extension of Forster's theory of long-range energy transfer to donor-acceptor pairs in systems of molecular dimensions *Z Phys Chem NF* **101**, 255—266
- Hof M (1990) Aufklärung schneller Prozesse in Flüssigkeiten, Gläsern und Membranen mittels zeitaufgelöster Fluoreszenzspektroskopie. Ph.D. Thesis Universität Würzburg
- Hof M, Schleicher J, Schneider F W (1989) Time resolved fluorescence in doped aerogels and organosilicate glasses. Bei Bunsenges *Phys Chem* **93**, 1377—1381
- John E, Jahng F (1991) Aggregation state of melittin in lipid vesicle membranes *Biochem Biophys J* **60**, 319—328
- Kanaoka Y, Machida M, Ban Y, Sekine T (1967) Fluorescence and structure of proteins as measured by incorporation of fluorophore. II. Synthesis of maleimide derivatives as fluorescence-labeled protein-sulphydryl reagents *Chem Pharm Bull Tokyo* **15**, 1738—1743
- Klafter J, Blumen A (1984) Fractal behavior in trapping and reaction *J Chem Phys* **80**, 875—877
- Klafter J, Blumen A (1985) Direct energy transfer in restricted geometries *J Luminescence* **34**, 77—82
- Kubitschek U, Kircheis M, Schweitzer-Stenner R, Dreybrodt W, Jovin M T, Pecht I (1991) Fluorescence resonance energy transfer on single living cells. Application to binding of monovalent haptens to cell-bound immunoglobulin E *Biochem Biophys J* **60**, 307—318
- Lawaczeck R, Gervais M, Nandi P K, Nicolau C (1987) Fusion of negatively charged liposomes with clathrin-uncoated vesicles *Biochim Biophys Acta* **903**, 112—122

- Murchie A I H, Clegg R M, Kitzing von E, Duckett D R, Diekmann S, Lilley D M J (1989) Fluorescence energy transfer shows that the four-way DNA junction is a right-handed cross of antiparallel molecules. *Nature (London)* **341**, 763—765
- Pitterich H, Lawaczeck R (1985) On the water and proton permeabilities across membranes from erythrocyte ghosts. *Biochim Biophys Acta* **821**, 233—242
- Rao A, Martin P, Reithmeier R A F, Cantley L C (1979) Location of the stilbenedisulfonate binding site of the human erythrocyte anion-exchange system by resonance energy transfer. *Biochemistry USA* **18**, 4505—4516
- Schwach G, Passow H (1978) Preparation and properties of human erythrocyte ghosts. *Mol Cell Biochem* **2**, 197—218
- Steck T L (1974) The organization of proteins in the human red blood cell membrane. A review. *J Cell Biol* **62**, 1—19
- Stein S, Bohlen P, Udenfriend S (1974) Studies on the kinetics of reaction and hydrolysis of fluorescamine. *Arch Biochem Biophys* **163**, 400—403
- Struck D K, Hoekstra D, Pagano R E (1981) Use of resonance energy transfer to monitor membrane fusion. *Biochemistry USA* **20**, 4093—4099
- Tamai N, Yamazaki T, Yamazaki I, Mizuma A, Mataga N (1987) Excitation energy transfer between dye molecules adsorbed on a vesicle surface. *J Phys Chem* **91**, 3503—3508
- Wolber P K, Hudson B S (1979) An analytical solution to the Forster energy transfer problem in two dimensions. *Biophys J* **28**, 197—210

Final version accepted January 20 1997